CHIN. PHYS. LETT. Vol. 33, No. 6 (2016) 064203

Creation of Super Long Transversely Polarized Optical Needle Using Azimuthally Polarized Multi Gaussian Beam

C. M. Sundaram[1], K. Prabakaran[2], P. M. Anbarasan[1], K. B. Rajesh[3**], A. M. Musthafa[4]

[1]*Department of Physics, Periyar University, Salem, Tamilnadu, India*
[2]*Department of Physics, Mahendra Arts and Science College (Autonomous), Namakkal, Tamilnadu, India*
[3]*Department of Physics, Chikkanna Government Arts College, Tiruppur, Tamilnadu, India*
[4]*Department of General Studies (Physics Group), Jubail University College (Male Branch), Royal Commission of Jubail, Kingdom of Saudi Arabia*

(Received 9 November 2015)

The intensity distribution in the focal region of a high-NA lens for the incident azimuthally polarized multi Gaussian beam transmitted through a multi belt spiral phase hologram is studied on the basis of the vector diffraction theory. Here we report a new method used to generate a needle of transversely polarized light beam with sub diffraction beam size of 0.366λ that propagates without divergence over a long distance of about 22λ in free space. We also expect that such a light needle of transversely polarized beam may find its applications in utilizing optical materials or instruments responsive to the transversal field only.

PACS: 42.25.Bs, 42.25.Ja, 42.79.Ag DOI: 10.1088/0256-307X/33/6/064203

In recent years, research interest in the tight focusing of light beams with radially and azimuthally electric field polarization has been increasing due to its unusual properties and the potential applications in the fields of optical data storage,[1–3] material processing,[4] optical coherence tomography,[5–7] lithography, and other uses. Such interest also arises from their other applications such as particle acceleration,[8–11] fluorescent imaging,[12] second-harmonic generation,[13–15] Raman spectroscopy,[16] high-resolution microscopy, and particle trapping. Recently, a subwavelength light needle with a super resolution was extensively investigated by using amplitude apertures,[17] phase apertures,[18] or their combination.[19,20] It was observed that a strong longitudinal component appears in the focal region of a tightly focused laser beam.[21–23] It also arises with focusing of radially polarized light.[24–26] Nevertheless, this longitudinally polarized beam is discontinuous at the interface of two neighboring media and enlarges the focusing spot in the high-NA medium. This implies that the subwavelength focused spot with longitudinal polarization is limited in applications such as imaging of silicon integrated circuits.[27,28] To solve this problem, suppression of longitudinal components by using an azimuthally polarized beam is suggested.[29] However, an azimuthally polarized focused beam generates a focal hole, and many novel methods are suggested to increase the focal depth of the focal hole.[30,31] Recently, it has been reported that this focal hole generated by an azimuthally polarized beam can be changed into a significantly sharper focal spot when a vortical phase is encoded on the azimuthally polarized beam, which shows the intriguing prospect in practical applications due to its subwavelength lateral spot size and the purely transverse electric field.[32] It is also proved that an annular azimuthally polarized beam with proper phase modulation can still achieve a further reduction (about 13.5%) to the spot area, compared with the radial polarization considered in previous studies. For some applications, it may be desirable to obtain a very narrow diffraction pattern with a tunable axial extent. For instance, in optical data storage, one would expect that the focal point possesses a small transverse dimension but a long focal depth;[33] this leads to a larger data density as well as a better tolerance for beam focusing. In biomedical imaging, temporal resolution is strongly enhanced by using beams with a long focal depth in two-photon laser scanning microscopy[34] or plane illumination microscopy.[35] More recently the generation of a non diffracting transversely polarized beam by highly focusing an azimuthally polarized BG beam with a high-NA lens and a multi-belt spiral phase hologram is demonstrated numerically.[36] It is reported that the beam propagates without divergence and its polarization remains almost invariant in the main lobe along the optical axis over a relatively long distance (∼4.84λ). Meanwhile, the formation of non-diffracting quasi-circularly polarized beams with a long depth of focus (DOF) (7.23λ) was shown by utilizing an amplitude modulated spiral phase hologram, by which similar transversal spot size (0.587λ) was generated.[37] In 2014, Nie *et al.* demonstrated the transversally polarized optical needle with focal spot 0.465λ with focal depth of 5.76λ using a complex filter.[38] In 2015, Lalithambigai *et al.* generated a subwavelength transversely polarized focal spot having an FWHM of 0.442λ with a long focal depth of 12.6λ using a phase modulated double ring shaped azimuthally polarized beam.[39] A multi belt phase modulation with a high-NA lens axicon is also proposed to generate a strong non-diffracting transversely polarized beam with the focal depth of about 11.4λ.[40] Recently, the radially polarized and amplitude-modulated annular multi Gaussian beam mode is proposed for illumi-

**Corresponding author. Email: rajeskb@gmail.com
© 2016 Chinese Physical Society and IOP Publishing Ltd

nating the pupil plane of the objective to achieve a sub wavelength longitudinal beam with a long focal depth.[38] In this Letter, we propose and demonstrate that a transversally polarized multi Gaussian beam with subwavelength (0.366λ) focal spot and relatively long focal depth ($\sim 22\lambda$) can be generated by highly focusing an azimuthally polarized multi Gaussian beam transmitted through a multi belt spiral phase hologram (MBSPH).

A schematic configuration of the proposed method is shown in Fig. 1. An incident azimuthally polarized multi Gaussian beam transmits through an MBSPH and is subsequently focused by a high-NA lens.

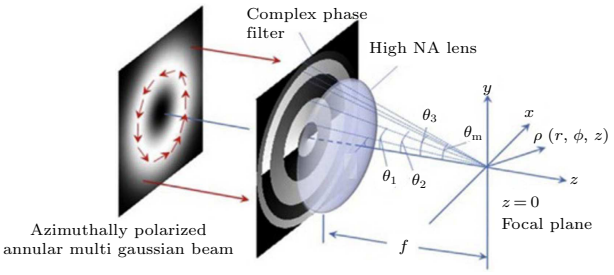

Fig. 1. Schematic diagram of the proposed system. The azimuthally polarized multi Gaussian beam passes through an MBSPH and is subsequently focused by a high-NA lens.

The analysis was performed on the basis of Richards' and Wolf's vectorial diffraction method widely used for high-NA focusing systems at arbitrary incident polarization.[42] In the case of the azimuthally incident polarization, adopting the cylindrical coordinates r, z, φ and the notations,[43] the electric field $E(r,\varphi,z)$ in the vicinity of the focal region reads

$$E(r,\varphi,z) = \begin{bmatrix} E_r \\ E_\varphi \\ E_z \end{bmatrix} = \begin{bmatrix} -Ae^{i\phi}(I_0 + I_2) \\ -Ae^{i\phi}(I_0 - I_2) \\ 0 \end{bmatrix}, \quad (1)$$

where

$$I_n = \int_0^{\theta_{\max}} \sqrt{\cos(\theta)} \cdot \sin(\theta) P(\theta) e^{ikz\cos\theta} J_n(kr\sin\theta) d\theta, \quad (2)$$

and A is the relative amplitude, $\theta_{\max} = \arcsin(\mathrm{NA}/n)$ is the maximum aperture angle with (NA/n) the ratio of numerical aperture (NA), n is the index of refraction between the lens and the sample, k is the wave number in free space, $e^{i\varphi}$ is the spiral phase mask (SPM), $J_n(\theta)$ denotes the nth-order Bessel function, and the function of $P(\theta)$ describes the amplitude modulation. For illumination by an annular multi Gaussian beam this function is given by[38]

$$P(\theta) = \left(\frac{\theta}{\theta_0}\right)^m \sum_{n=-N}^{N} \exp\left[-\left(\frac{\theta - \theta_c - n\omega_0}{\omega_0}\right)^2\right], \quad (3)$$

where θ is the converging semi-angle. We denote the maximum converging semi-angle as $\theta_{\max}$, which is related to the objective numerical aperture by $\theta_{\max} = \arcsin(\mathrm{NA})$, θ_0 is an angle which, along with integer m, determines the shape of the modulation function, θ_0 is usually chosen to be slightly smaller than $\theta_{\max}$, and θ_c determines the radial position translation of $P(\theta)$. We take $\theta_c = \theta_{\max}/2$. Here ω_0 is the waist width of the single Gaussian beam calculated by

$$\omega_0 = \frac{1}{2} \frac{\theta_{\max}}{N + \{1 - \ln[\sum_{n=-N}^{N} \exp(-n^2)]\}^{1/2}}. \quad (4)$$

Equation (3) describes an object beam. It is suitable to convert Eq. (1) from a function of angle into a function of radial polar coordinate. One may substitute θ with $\arcsin(r/f)$, where f is the focal distance of the objective. In Eq. (3), the factor (θ/θ_0) measures that most of the light energy is located on the annular edge of the pupil. Increasing the integer m concentrates more energy into the annular edge area in which the converging semi-angle is more than θ_0. The sum of $(2N+1)$ spatially equally spaced Gaussian beams ensures that the amplitude of the constructed annular multi Gaussian beam decreases suddenly, when reaching the outer edge of the pupil. Such an amplitude modulated beam can be realized by encoding a suitable phase mask on a spatial light modulator. In the following simulation calculations, the coordinates in all the figures are in units of the wavelength.

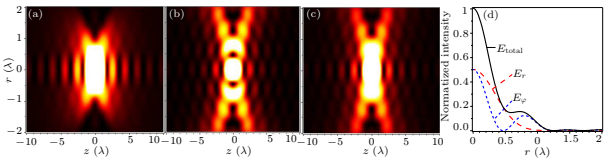

Fig. 2. The contour plots of the azimuthally polarized beam focused by high-NA lens. The intensity profiles of (a) radial, (b) azimuthal and (c) total intensity distribution components of the optical field at near the focal plane for NA = 0.9.

We perform the integration of Eq. (1) numerically using parameters $\lambda = 1$ and $\mathrm{NA} = 0.9$. Here for simplicity, we assume the refractive index $n = 1$, $A = 1$ and $m = 30$. For all the calculation the length unit is normalized and the energy density is normalized to unity. The intensity profiles of the radial component, the azimuthal component, and the total field of the azimuthally polarized beam in the focal region are illustrated in Fig. 2 and are in good agreement with Fig. 2 of Ref. [36]. Figures 3(a)–3(c) illustrate the evolution of three-dimensional intensity distribution of radial component, azimuthal component and total intensity of the high-NA lens in the r–z plane for the incident azimuthally polarized multi Gaussian beam (MGB) with ordinary spiral phase hologram (without the multi belt structure).

It can be seen that the DOF is about 10.36λ with nearly uniform axial intensity distribution. From Figs. 3(d) and 3(c) we can measure that the radial component is 50% of the total intensity, FWHM of the generated focal spot is 0.39λ, and its focal depth is 10.36λ. Based on the explicit formula given in Eq. (1),

we aim to achieve a long focal depth transversally polarized beam. We show that this is possible to carry out with additional phase modulation. A schematic diagram of the suggested method is shown in Fig. 1. A four-belt complex filter modulated spiral phase filter is placed at the pupil plane, where the transmissions from the inner to the outer zones are 0, 1, 0, and −1, respectively.

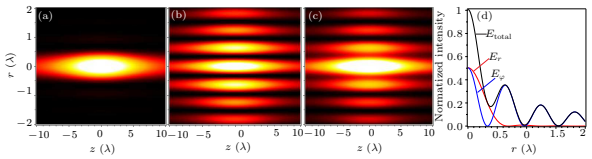

Fig. 3. The contour plots of the azimuthally polarized multi Gaussian beam focused by high-NA lens. The intensity profiles of (a) radial, (b) azimuthal and (c) total intensity distribution components of the optical field at near the focal plane, and (d) 2D intensity distribution for $m = 30$.

The effect due to the interference of the second and fourth zones of the MBSPH on the input azimuthally polarized multi Gaussian beam is evaluated by replacing the function $P(\theta)$ with the function $P(\theta)\times$MBSPH where MBSPH(θ) is given by

$$\text{MBPSH}(\theta) = \begin{cases} 0, & \text{for } 0 < \theta < \theta_1, \theta_2 < \theta < \theta_3, \\ 1, & \text{for } \theta_1 < \theta < \theta_2, \\ -1, & \text{for } \theta_3 < \theta < \theta_{\max}. \end{cases} \tag{5}$$

We observed that it is possible to generate sub wavelength focal spot segment by properly constructing the MBSPH for the incident azimuthally polarized multi Gaussian beam. We choose one structure with random values for θ_1–θ_3 from all possibilities and simulate their focusing properties by the vector diffraction theory. As an example, the set of three angles optimized for uniform sub wavelength focal spot segments are $\theta_1 = 31.48°$, $\theta_2 = 54.12°$, $\theta_3 = 61.37°$ and $\theta_{\max} = 64.19°$, respectively. Figure 4 shows the focal structure obtained for the above-mentioned MBSPH. From Fig. 4(a), we observed that the proposed MBSPH confines the radial component and extends focal depth, and Fig. 3(b) shows that the azimuthal component is scattered away from the focal line and results in the formation of side lobes with ∼34% of the total intensity distribution.

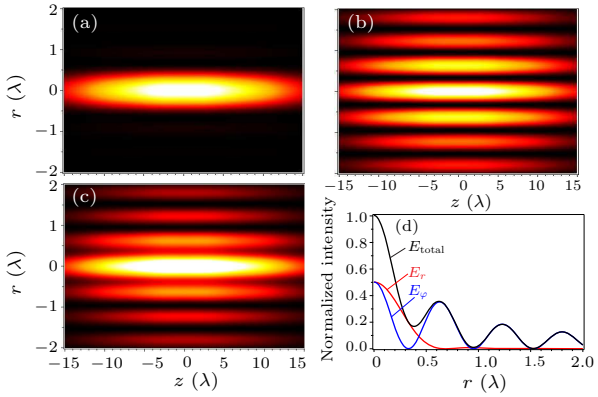

Fig. 4. The contour plots of the phase modulated azimuthally polarized multi Gaussian beam focused by high-NA lens. The intensity profiles of (a) radial, (b) azimuthal and (c) total intensity distribution components of the optical field at near the focal plane, and (d) 2D intensity distribution for $m = 30$.

The total intensity distribution shown in Fig. 4(c) reveals that the focal segment generated by the proposed MBSPH contains sub wavelength focal spot with a large focal depth. From Fig. 4(d), we measure the FWHM of the focal spot to be 0.366λ. From Fig. 4(c), we measure its corresponding focal depth to be 22λ. The depth of focus (DOF) of the focal spot generated by our method extends over 10 times of that mentioned in recent works.[36–40] This result is also better than other methods mentioned before. Table 1 lists the comparison of FWHM of the focal spot and its corresponding focal depth generated by the high-NA lens system under different methods.

Table 1. The performances of diverse methods.

Method	Spot size (λ)	Depth of focus (λ)
Without phase modulation[36]	0.54	1.2
Seven-zone complex spiral phase[38]	0.465	5.76
Azimuthally polarized beam Laguerre Gaussian with complex spiral phase mask[39]	0.442	12.6
Azimuthally polarized Bessel Gaussian beam with five belt binary optical method[40]	0.384	11.45
Proposed method	0.366	22

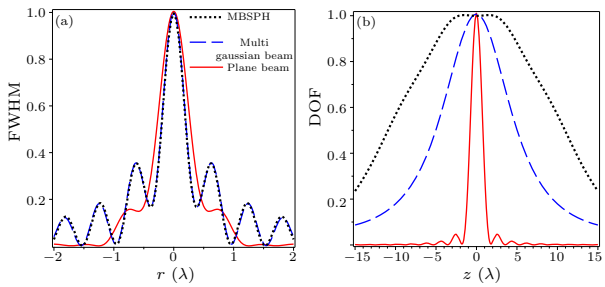

Fig. 5. Normalized two-dimensional total electric field intensity distributions (a) along the transverse direction and (b) along the axial direction.

Figures 5(a) and 5(b) show the normalized comparison plot of the total electric field along the transverse and axial directions. From Fig. 5(a), we measure that the total spot size is reduced to 0.366λ (black dashed line) and gives a sub wavelength focal depth 22λ (black dashed line) as shown in Fig. 5(b).

By calculating the Stokes parameter, the azimuthal angle ψ and ellipticity $\tan\chi$ of the polarization ellipse can be derived by using

$$\tan(2\psi) = S_2/S_1 = \tan[2\phi + \arg(I_0^* I_2)], \tag{6}$$

$$\sin(2\chi) = S_3/S_0 = (|I_0|^2 - |I_2|^2)/(|I_0|^2 - |I_2|^2), \tag{7}$$

where S_i describes the Stokes polarization vector component, the superscript $*$ denotes the complex con-

jugate, and the argument gives the argument of the complex number x. Figure 6 shows the ellipticities of the local polarization ellipses at different axial positions. It is noted that the polarization has no apparent change within the DOF. This reveals that the polarization of the non-diffracting beam keeps almost invariant within the DOF range. It is also noted that as the radial distance increases, the ellipticity decreases rapidly from 1 to 0, where it changes the handedness from right-hand polarization to left-hand polarization. The above simulation calculations show that, by utilizing the MBSPH to modulate the phase of azimuthally polarized multi Gaussian beam, the optical spot in the focal region can be used as a powerful tool for particle manipulation. It is a simple and flexible method of forming sub wavelength focal spot with a large focal depth. The work is important for nanoscale imaging, nanolithography, trapping, manipulating particles, etc.

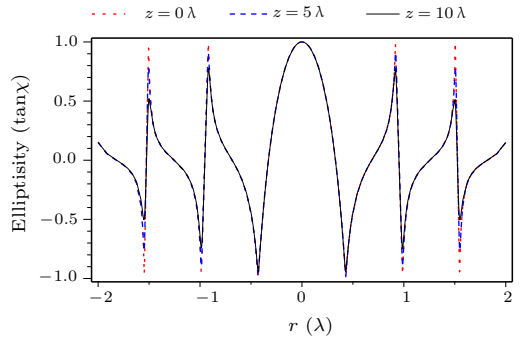

Fig. 6. (Color online) Cross section of the ellipticity of local polarization ellipses at different observation planes.

In conclusion, the proposed multi belt phase modulation with high-NA lens to generate a needle of transversely polarized beam by focusing an azimuthally polarized multi Gaussian beam has been analyzed and demonstrated numerically by using the vector diffraction theory. The proposed method generates a sub wavelength transversely polarized focal spot having FWHM of 0.366λ with long focal depth of 22λ. Such an investigation is worthwhile for potentially using in optical trapping and optical microscopy, optical micromachining and photolithography.

References

[1] Wang H F, Shi L P, Lukyanchuk B, Sheppard C, Chong C T 2008 *Nat. Photon.* **2** 501
[2] Wang H F, Shi L P, Yuan G Q, Miao X S, Tan W L and Chong C T 2006 *Appl. Phys. Lett.* **89** 171102
[3] Sun C C and Liu C K 2003 *Opt. Lett.* **28** 99
[4] Erdélyi M, Horváth Z L, Szabó G, Bor S, Tittel F K, Cavallaro J R and Smayling M C 1997 *J. Vac. Sci. Technol.* B **15** 287
[5] Liu L B, Liu C, Howe W C, Sheppard C J R and Chen N G 2007 *Opt. Lett.* **32** 2375
[6] Leitgeb R A, Villiger M, Bachmann A H, Steinmann L and Lasser T 2006 *Opt. Lett.* **31** 2450
[7] Zhang Q Q, Wang J G, Wang M W, Bu J, Zhu S W, Wang R, Gao B Z and Yuan X C 2011 *J. Opt.* **13** 055301
[8] Cicchitelli L, Hora H and Postle R 1990 *Phys. Rev.* A **41** 3727
[9] Fontana J R and Pantell R H 1983 *J. Appl. Phys.* **54** 4285
[10] Romea R D and Kimura W D 1990 *Phys. Rev.* D **42** 1807
[11] Rosenzweig J, Murokh A and Pellegrini C 1995 *Phys. Rev. Lett.* **74** 2467
[12] Novotny L, Beversluis M R, Youngworth K S and Brown T G 2001 *Phys. Rev. Lett.* **86** 5251
[13] Bouhelier A, Beversluis M, Hartschuh A and Novotny L 2003 *Phys. Rev. Lett.* **90** 013903
[14] Biss D P and Brown T G 2003 *Opt. Lett.* **28** 923
[15] Yew E Y S and Sheppard C J R 2007 *Opt. Commun.* **275** 453
[16] Hayazawa N, Saito Y and Kawata S 2004 *Appl. Phys. Lett.* **85** 6239
[17] Sheppard C J R and Choudhury A 2004 *Appl. Opt.* **43** 4322
[18] Helseth L E 2001 *Opt. Commun.* **191** 161
[19] Liu C and Park S H 2004 *Opt. Lett.* **29** 1742
[20] Xu Y, Singh J, Sheppard C J R and Chen N 2007 *Opt. Express* **15** 6409
[21] Sheppard C J R 1978 *IEE J. Microwaves Opt. Acoust.* **2** 163
[22] Ganic D, Gan X S and Gu M 2003 *Opt. Express* **11** 2747
[23] Lee K G and Kihm H W 2007 *Nat. Photon.* **1** 53
[24] Bouchal Z and Olivik M 1995 *J. Mod. Opt.* **42** 1555
[25] Sheppard C J R and Török P 1997 *Optik* **104** 175
[26] Sheppard C J R and Saghafi S 1999 *Opt. Lett.* **24** 1543
[27] Huang K, Ye H, Liu H, Teng J, Yeo S P and Qiu C W 2014 arXiv:1406.3823
[28] Qin F, Huang K, Wu J, Jiao J, Luo X, Qiu C and Hong M 2015 *Sci. Rep.* **5** 1
[29] Machavariani G and Lumer Y 2007 *Opt. Lett.* **32** 1468
[30] Lalithambigai K, Suresh P, Ravi V, Prabakaran K, Jaroszewicz Z, Rajesh K B, Anbarasan P M, Pillai T V S 2012 *Opt. Lett.* **37** 99
[31] Tian B and Pu J X 2011 *Opt. Lett.* **36** 2014
[32] Hao X, Kuang C F, Wang T T and Liu X 2010 *Opt. Lett.* **35** 3928
[33] Grosjean T, Courjon D and Bainier C 2007 *Opt. Lett.* **32** 976
[34] Dufour P, Piché M, De Koninck Y and McCarthy N 2006 *Appl. Opt.* **45** 9246
[35] Planchon T A, Gao L, Milkie D E, Davidson M W, Galbraith J A, Galbraith C G and Betzig E 2011 *Nat. Methods* **8** 417
[36] Yuan G H, Wei S B and Yuan X C 2011 *Opt. Lett.* **36** 3479
[37] Yuan G, Wei S and Yuan X 2011 *J. Opt. Soc. Am.* A **28** 1716
[38] Nie Z, Li Z, Shi G, Zhang X, Wang Y and Song Y 2014 *Opt. Lasers Eng.* **59** 93
[39] Lalithambigai K, Anbarasan P M and Rajesh K B 2015 *Opt. Quantum Electron.* **47** 1027
[40] Suresh P, Mariyal C, Rajesh K B, Pillai T V S and Jaroszewicz Z 2013 *Appl. Opt.* **52** 849
[41] Chen J N, Xu Q F and Wang G 2011 *Chin. Phys.* B **20** 114211
[42] Youngworth K S and Brown T G 2000 *Opt. Express* **7** 77
[43] Richards B and Wolf E 1959 *Proc. R. Soc. London* A **253** 358
[44] Collet E 1993 *Polarized Light* (New York: Marcel Dekker)
[45] Bomzon Z, Gu M and Shamir J 2006 *Appl. Phys. Lett.* **89** 241104